Amnionless function is required for cubilin brush-border expression and intrinsic factor-cobalamin (vitamin B_{12}) absorption in vivo

Qianchuan He, Mette Madsen, Adam Kilkenney, Brittany Gregory, Erik I. Christensen, Henrik Vorum, Peter Højrup, Alejandro A. Schäffer, Ewen F. Kirkness, Stephan M. Tanner, Albert de la Chapelle, Urs Giger, Søren K. Moestrup, and John C. Fyfe

Amnionless (AMN) and cubilin gene products appear to be essential functional subunits of an endocytic receptor called cubam. Mutation of either gene causes autosomal recessive Imerslund-Gräsbeck syndrome (I-GS, OMIM no. 261100) in humans, a disorder characterized by selective intestinal malabsorption of cobalamin (vitamin B_{12}) and urinary loss of several specific low-molecular-weight proteins. Vital insight into the molecular pathology of I-GS has been obtained from studies of dogs with a similar syndrome. In this work, we show that I-GS segregates in a large canine kindred due to an in-frame deletion of 33 nucleotides in exon 10 of *AMN*. In a second, unrelated I-GS kindred, affected dogs exhibit a homozygous substitution in the *AMN* translation initiation codon. Studies in vivo demonstrated that both mutations abrogate AMN expression and block cubilin processing and targeting to the apical membrane. The essential features of AMN dysfunction observed in vivo are recapitulated in a heterologous cell-transfection system, thus validating the system for analysis of AMN-cubilin interactions. Characterization of canine *AMN* mutations that cause I-GS establishes the canine model as an ortholog of the human disorder well suited to studies of AMN function and coevolution with cubilin. (Blood. 2005;106:1447-1453)

Introduction

Adult-onset gastrointestinal malabsorption of the essential micronutrient, cobalamin (vitamin B_{12}), leads to potentially lethal manifestations as diverse as megaloblastic anemia and neutropenia, degeneration of spinal cord nerve tracts, and dementia.[1] In the very young, signs of cobalamin malabsorption may also include growth retardation or loss of developmental milestones or both. Imerslund-Gräsbeck syndrome (I-GS; also called megaloblastic anemia 1, OMIM no. 261100) is an autosomal recessive disorder characterized by selective malabsorption of cobalamin in the intestine and, most often, of specific low-molecular-weight proteins in renal proximal tubules.[2,3] Patients with I-GS typically present at 2 to 4 years of age with signs of cobalamin deficiency and proteinuria. More than 200 human cases and familial clusters have been reported in Finland, Norway, the Middle East, and Northern Africa.[1] Various null and missense mutations of the cubilin (*CUBN*) [4] and amnionless (*AMN*) genes[5] have been implicated in I-GS kindreds, but both loci have been excluded in some.[6] In addition, a number of patients suffering from gastric intrinsic factor (IF) deficiency have been misdiagnosed as having I-GS.[7]

Cubilin is a 460-kDa multiligand receptor protein that mediates endocytosis of the IF-cobalamin complex from distal small intestinal chyme and of several proteins from glomerular filtrate in renal proximal tubules.[8] AMN is an approximately 48-kDa apical membrane protein also expressed in intestinal and proximal tubule epithelia but whose function is poorly defined.[5,9] Recent studies suggested that cubilin and AMN function as subunits of a receptor complex, now called "cubam."[10] However, no studies have directly assessed the effect of *CUBN* or *AMN* mutations on cubam expression in patients with I-GS because these proteins are expressed in inaccessible tissues, and the clinical disease is easily treated. Unfortunately, the AMN knockout mouse exhibits an embryonic lethal phenotype.[9]

Canine I-GS was derived originally from purebred giant schnauzers (GSs) as a naturally occurring animal model of the human disorder[11-13] and has contributed significantly to understanding of its molecular biologic basis as well as aspects of cubilin function.[14-17] *CUBN* was excluded from the GS disease locus,[18] and the disorder was recently mapped to an approximately 4-Mb interval predicted to harbor *AMN*.[19] To define the molecular basis of the canine I-GS model, we sought *AMN* mutations segregating in the GS kindred and an unrelated kindred of Australian shepherd (AS) dogs and investigated in vivo AMN and cubilin expression in affected dogs. Additionally, comparison of these results to expression of mutant canine *AMN* in a heterologous mammalian-cell transfection system validates the cell-culture system for ex vivo

From the Department of Microbiology and Molecular Genetics, College of Veterinary Medicine, Michigan State University (MSU), East Lansing, MI; Department of Medical Biochemistry, University of Aarhus, Aarhus, Denmark; Department of Cell Biology, Institute of Anatomy, University of Aarhus, Aarhus, Denmark; Department of Biochemistry and Molecular Biology, Odense University, Odense, Denmark; National Center for Biotechnology Information, National Institutes of Health, Department of Health and Human Services, Bethesda, MD; Institute for Genomic Research, Rockville, MD; Human Cancer Genetics Program, Comprehensive Cancer Center, Ohio State University, Columbus, OH; and Section of Medical Genetics, Veterinary Hospital of the University of Pennsylvania, Philadelphia, PA.

Submitted March 24, 2005; accepted April 13, 2005. Prepublished online as *Blood* First Edition Paper, April 21, 2005; DOI 10.1182/blood-2005-03-1197.

Supported in part by the National Institutes of Health (grants DK064161, RR02512, and CA16058), the Michigan State University Companion Animal Fund, and the Howard Hughes Undergraduate Research Scholars Program (A.K.). Part of this study was prepared under a grant from the State of Ohio Biomedical Research and Technology Transfer Commission (reflecting the views of the grantees, not necessarily of the granting agency).

An Inside *Blood* analysis of this article appears in the front of the issue.

Reprints: John C. Fyfe, 2209 Biomedical and Physical Sciences, Michigan State University, East Lansing, MI 48824; e-mail: fyfe@cvm.msu.edu.

The publication costs of this article were defrayed in part by page charge payment. Therefore, and solely to indicate this fact, this article is hereby marked "advertisement" in accordance with 18 U.S.C. section 1734.

determination of functional domains in both proteins and defects caused by *CUBN* and *AMN* mutations.

Materials and methods

Animals

Dogs were handled according to principles and protocols approved by the MSU All University Committee for Animal Use and Care. MSU University Laboratory Animal Resources housed dogs of the GS kindred. Private owners submitted samples for DNA isolation from dogs of the AS kindred. DNA samples of 80 unrelated healthy dogs of 10 various breeds were a kind gift from V. Yuzbasiyan-Gurkan (MSU). DNA of additional healthy dogs was isolated from anonymous blood samples submitted to the MSU Veterinary Clinical Pathology Laboratory.

Linkage analysis and AMN cDNA cloning

gDNA was prepared variously from buccal brushes, blood, or frozen liver by standard methods.[20,21] Canine sequences of the kinesis 2 gene (*KNS2)* were obtained from a database of genomic sequence maintained by The Institute for Genomic Research as described previously.[19] Part of *KNS2* was amplified from gDNA using polymerase chain reaction (PCR) primers 5′-GAGCCTCTGGATGACCTTTTC-3′ and 5′-CACTGCTATGCTGCTGTTGGACT-3′, and a C>T polymorphism was identified (CFA 8, position 74340382, July 2004 canine genome assembly). *KNS2* genotyping was by direct sequencing of PCR products, and linkage analysis was with the FASTLINK software package, version 4.1P (NCBI, Bethesda, MD).[22-24] DNA was sequenced by automated dideoxy chain termination technology (University of Michigan DNA Sequencing Core Facility, Ann Arbor, MI).

A canine proximal tubule cell cDNA bacteriophage λ library[25] was screened by pooled PCR selection[26] amplifying a portion of *AMN* cDNA using primers 5′-TCTTCTYCGTGGACGCCGAGCG-3′ and 5′-GGTCCTCGTCGCGCGWGAACGT-3′. After phage purification, clones were rescued into the phagemid pBluescript (Stratagene, La Jolla, CA). Inserts were sequenced completely on both strands and analyzed using Lasergene software (DNAstar, Madison, WI). The full-length canine *AMN* cDNA sequence was submitted to the EMBL/GenBank Data Libraries (accession no. AY368152).

AMN expression analysis

RNA was isolated and Northern blots were prepared as described previously[13] using a random primed-labeled *AMN* cDNA probe. *AMN* expression was examined in various tissues by reverse transcription-coupled PCR (RT-PCR) with PCR primers 5′-CGGGCGCGCGGCGGGATG-3′ and 5′-CTGGCCAGCCCCGCGGTTGC-3′ to amplify the full-length cDNA. Primers for *CUBN* cDNA (exons 8-12) detection in the same RT reactions were 5′-AGCCTGCGTGCTGGACATAGAC-3′ and 5′-CCAGCCCAACCTGATTCACACTTA-3′ and for *PPID* (peptidyl-prolyl isomerase D, also called cyclophilin D) cDNA (exons 3-7) detection were 5′-TCAGGGTGGAGACTTCTCAAATC-3′ and 5′-GTTGCAGCTTCAGTCTATCTGCT-3′.

Anti–canine AMN peptide antisera were produced by immunizing rabbits with synthetic peptides TARESGAPVGDGSA (AMN residues 340-353) and RRAPRLRWTKRER (residues 388-400) in the custom antibody production facilities of ProSci (Poway, CA) under the National Institutes of Health Animal Welfare Assurance (no. A4182-01). IF-cobalamin–binding proteins were isolated in the presence of a protease inhibitor cocktail from membrane or supernatant fractions of kidney homogenates[27] produced from tissue that was snap-frozen in liquid nitrogen immediately after the dogs were humanely killed; proteins were stored at −80°C. Endoglycosidase H (endo H) and peptide N-glycosidase F (PNGase F) digestions were carried out essentially as described previously.[10,13] Proteins were separated variously by reducing sodium dodecyl sulfate–polyacrylamide gel electrophoresis (SDS-PAGE) or by 2-dimensional gel electrophoresis (nonlinear pH 3-10 isoelectric focusing and reducing SDS-PAGE on 15% gels).[28] Gels were silver stained[29] or blotted to polyvinylidene difluoride (PVDF) membranes. Immunoblots were incubated as previously described[10,13] with anti–AMN peptide sera diluted 1:40 000. Secondary antibody was anti–rabbit IgG–alkaline phosphatase conjugate (Sigma, St Louis, MO), and proteins were detected with *P*-nitroblue tetrazolium/5-bromo-4-chloro-3-indolyl phosphate. Specificity of primary antisera was determined on control blots incubated with decreasing concentrations of the primary anti-AMN sera, preimmune sera, sera depleted of specific antibody by peptide affinity chromatography, or secondary antibody only.

Bands or spots separated by SDS-PAGE or 2-dimensional gel electrophoresis and corresponding to immunodetected proteins were subjected to in-gel tryptic digestion followed by liquid chromatography coupled with tandem mass spectrometric peptide mapping (LC/MS/MS) in the Proteomics Core of the MSU Genomics Technology Support Facility, as previously described.[30] Resulting spectra were searched against the NCBInr database, using the Mascot searching algorithm (Matrix Science, Boston, MA) with taxonomy limited to mammals.[31] The respective probability-based molecular weight search (Mowse) scores for the approximately 48-kDa and approximately 40-kDa canine AMN species were 1038 and 657.

Mutation determination

Kidney cortex RNA of dogs was isolated and RT reactions were performed as before. PCR amplification of RT products was with primers described (see "*AMN* expression analysis") for full-length *AMN* cDNA amplification or, to examine the translation initiation sequence, with primers 5′-CGGGCGCGCGGCGGG-3′, the 15 bp immediately 5′ of the translation initiation codon, and 5′-CGCTCGGCGTCCACGGAGAAGA-3′ in exon 5. cDNA amplification products were sequenced, and putative mutations were confirmed by PCR amplification of gDNA. Screening for the c.1113_1145del allele in the GS kindred and unrelated populations was by PCR amplification of gDNA templates using primers 5′-TCCGTTGCAGGCGAAGCCCTC-3′ and 5′-CTGCGGGGTGCGTGGAACCTAG-3′. Allele-specific products were separated by agarose electrophoresis in 2% gels. Screening for the c.3G>A allele in the AS kindred and unrelated populations was by PCR, using primers 5′-GGCTTGGAAGGAAGGCCCCCA-3′ and 5′-CAAGGCGGGGAGCCTCCGAA-3′, followed by *Bst*F5I digestion of the products and electrophoresis of the allele-specific digestion products on 2.5% gels.

Analysis of AMN and cubilin expression in affected dogs in vivo

Membrane and soluble fraction proteins of healthy and GS kindred affected dogs were isolated in parallel, each from 125 g kidney cortex, by IF-cobalamin affinity chromatography as previously described.[10,27] One- and 2-dimensional SDS-PAGE gels were prepared and protein bands or spots between 37 and 50 kDa observed on gels of healthy dog proteins, but not on the corresponding gels of affected dog proteins, were identified by LC/MS/MS peptide mapping and Western blotting as described (see "*AMN* expression analysis").

For biopsy quantities of tissue (< 1 g), kidney cortex was thawed and homogenized in 9 volumes of cold 50 mM Tris (tris(hydroxymethyl)aminomethane–Cl (pH 7.4) containing 150 mM NaCl, 1 mM *N*-ethyl maleimide, 5 mM phenylmethylsulfonyl fluoride, and 2 mM EDTA (ethylenediaminetetraacetic acid). Homogenates was incubated for 2 hours at 4°C, with constant agitation, after 3-[(3-cholamidopropyl)dimethylammonio]-1-propanesulfonate (CHAPS) was added to 0.6%. Rat gastric IF-cobalamin beads were prepared as previously described.[13] Detergent extracts were centrifuged at 4°C for 40 minutes at 40 000*g*, and supernatant aliquots containing 100 mg total protein were made 5 mM $CaCl_2$ and incubated with 20 μL rat IF-cobalamin beads overnight at 4°C. The beads were washed 3 times in homogenization buffer without EDTA containing 0.6% CHAPS, boiled in gel-loading buffer, and subjected to reducing SDS-PAGE and immunoblotting as described (see "*AMN* expression analysis").

For immunohistochemistry, sections of normal and affected dog kidney cortex were fixed by perfusion of the renal artery with phosphate-buffered 4% paraformaldehyde, sliced to 1.5-mm thickness, and immersed for 48 hours in phosphate-buffered 1% paraformaldehyde. Thin sectioning and peroxidase-labeled immunostaining for light microscopy was performed as previously described.[16] Primary antibody was a previously described[13,16]

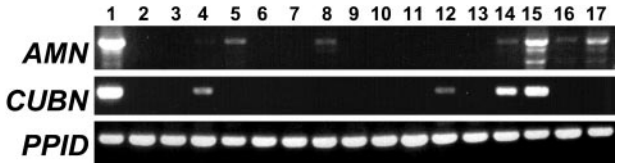

Figure 1. Tissue expression *AMN* and *CUBN* cDNA. Total RNA isolated from the designated tissues was amplified by RT-PCR. *AMN* primers were designed to amplify the full-length coding sequence (product size 1.4 kbp). *CUBN* primers amplified exons 8-12 (product size 0.5 kbp). *PPID* primers were used as a positive control for success of the RT reaction in each RNA sample (product size 0.6 kbp). Lanes: 1, kidney; 2, muscle; 3, spleen; 4, thymus; 5, liver; 6, heart; 7, lung; 8, pituitary; 9, testis; 10, cerebellum; 11, cerebrum; 12, placenta; 13, duodenum; 14, jejunum; 15, ileum; 16, colon; 17, pancreas.

rabbit polyclonal anti–canine cubilin serum (1:4000) that did not cross-react with AMN. None of the anti–human, anti–mouse, or anti–canine AMN peptide antisera produced to date detected AMN specifically in canine tissue sections. Stained tissues were examined by light microscopy (Leica DMR microscope with 40×/0.70 numerical aperture objective attached to a Leica DFC320 camera [Leica Microsystems, Wetzlar, Germany]). Images were produced digitally with Leica DFCT Twain 6.1.0 acquisition software and Adobe Photoshop 8.0 (Adobe Systems, San Jose, CA).

Mutation analysis in transfected CHO cells

Open reading frames of normal canine *AMN* and c.1113_1145del *AMN* cDNAs were amplified by PCR from plasmid templates using primers that incorporated *Hind*III recognition sites, cloned into the pCR 2.1-TOPO plasmid (Invitrogen, Carlsbad, CA), and fully sequenced to confirm integrity of the insert. After digestion with *Hind*III, purified insert DNA was ligated into the previously described pcDNA3-5*Myc* plasmid expression vector.[5] Stable, double-transfected CHO lines expressing a "mini-cubilin" construct (amino acids 1-1389 of rat cubilin) and the normal or mutant canine *AMN*-5*Myc* constructs were established and maintained as described before.[10] Expression products in CHO lysates were analyzed by immunoblotting using rabbit polyclonal antibody against rat cubilin and an anti-myc antibody (Invitrogen) for AMN detection. For endo H digestion, cyanogen bromide (CNBr)–activated Sepharose 4B beads (Amersham Biosciences, Arlington Heights, IL) coupled with porcine IF-cobalamin as previously described[27] were incubated with lysates for pull-down of recombinant cubilin. The beads were washed and subjected to endo H (Roche, Indianapolis, IN) digestion as previously described[10,12] prior to SDS-PAGE and immunoblotting.

Immunofluorescent analysis of cubilin-expressing CHO cell lines transfected with normal or mutant *AMN* was performed on living, nonpermeabilized cells as previously described.[10] Briefly, living cells were incubated for 90 minutes at 4°C with a polyclonal rabbit antibody against rat cubilin (diluted to 10 μg/mL in growth medium) and then fixed in 10 mM phosphate-buffered saline (PBS) containing 4% formaldehyde for 1 hour at 4°C. Finally, the cells were incubated for 1 hour at room temperature with Alexa Fluor 488-labeled goat antirabbit antibody (Molecular Probes, Eugene, OR) diluted 1:200. Stained cells were examined by laser scanning confocal fluorescence microscopy under water (Zeiss LSM 510 confocal system attached to an Axiovert microscope with a 63×/1.2 numeral aperture plan C-Apochromat objective and optical magnification of 63 × 10 [Carl Zeiss, Oberkochen, Germany]). Images were produced digitally with Zeiss LSM 510 software and Adobe Photoshop 5.0.

Results

AMN expression analysis

The cloned full-length canine *AMN* cDNA (GenBank accession no. AY368152) was 77% GC and composed of a 15-bp 5′-untranslated region (UTR), 1374 bp of open reading frame, and 152 bp of 3′-UTR that included a single polyadenylation signal 11 bp 5′ of the poly A tract. The deduced amino acid sequence of 458 residues was 73%, 66%, 65%, 38%, 34%, 33%, and 21% identical to AMN of human (NP112205), mouse (NP291081), rat (XP234547), chicken (XP421397), *Xenopus lavis* (AAH74152), puffer fish (Fugu chrUn:215972629-215974032; UCSC Genome Browser, August 2002 assembly) and fruit fly (NP608515), respectively. Structural features conserved among these species included the predicted signal sequence cleavage site (after Ala19); 12 cysteine residues in the mature extracellular domain with 9 clustered in a cysteine-rich domain between residues 205-253; a single, similarly placed transmembrane domain (residues 363-387 of dog AMN); and 2 copies of [FY]XNPX[FY], a well-characterized signal for ligand-independent receptor internalization via clathrin-coated pits.[32] Potential asparagine (N)–linked glycosylation sites (dog residues 35 and 39) were found within the first 40 amino acid residues of the protein in all but the chicken and fruit fly sequences.

Northern blot of canine kidney RNA revealed a single *AMN* transcript of about 1.5 kbp. RT-PCR demonstrated full-length *AMN* mRNA as expected in tissues of known *CUBN* expression, inclu ding kidney cortex, jejunum, and ileum (Figure 1). cDNA of both genes was also detected in thymus but at very low levels. In addition, *AMN* but not *CUBN* cDNA was expressed in colon, liver, pancreas, and pituitary, and *CUBN* but not *AMN* cDNA was expressed in placenta.

Western blotting with antiserum raised against an extracellular domain peptide of canine AMN (Figure 2 lane 1) demonstrated 3 immunospecific proteins (approximate molecular masses of 40, 43, and 48 kDa) in renal cortex membranes isolated from fresh-frozen tissue. Each had approximately 3 kDa of N-linked oligosaccharide as demonstrated by PNGase F digestion (Figure 2 lane 2). The 3 isoforms exhibited varying isoelectric points at about pH 8.5 to 9 determined in the first dimension of 2-dimensional gel electrophoresis (Figure 2 lane 4). Peptide mapping of the approximately 40-kDa protein isolated by 2-dimensional gel electrophoresis identified AMN peptides of residues 41-54, 62-73, 74-92, 93-109, 126-134, 139-151, 165-175, 176-186, 192-199, and 277-291, composing 38% of the protein extracellular domain. None of the observed peptides mapped to the transmembrane or intracellular domains. Consistent with this was that the approximately 40-kDa band was not detected on Western blots using an anti–canine AMN serum directed at a peptide of the intracellular tail (Figure 2 lane 3) and

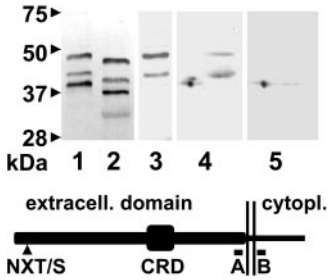

Figure 2. Immunodetection and characterization of AMN in canine kidney. AMN was enriched from membrane (lanes 1-4) or supernatant (lane 5) fractions of homogenates of normal dog kidney cortex by IF-cobalamin affinity column chromatography. Eluted proteins were separated by SDS-PAGE (lanes 1-3) or by 2-dimensional gel electrophoresis (blots 4 and 5). Proteins in lanes 1 and 2 were subjected to mock and PNGase F digestion, respectively, prior to electrophoresis and blotting. The additional, lightly stained band in lane 2 migrates at the expected position of PNGase F. Antiserum against the extracellular domain peptide A, as shown in the schematic, was used for immunodetection in 1, 2, 4, and 5, and antiserum against the cytoplasmic domain peptide B was used in lane 3. The schematic of the mature, full-length AMN protein indicates the relative positions of the site of N-linked oligosaccharide addition (NXT/S), the cysteine-rich domain (CRD), and peptides A (amino acid residues 340-353) and B (residues 388-400) against which antisera were raised. The excess positive charge of the intracellular domain protein sequence including peptide B is + 3. Two vertical lines indicate the single transmembrane domain.

that the small isoform exhibited a more acidic isoelectric point than the 2 larger species. Furthermore, the approximately 40-kDa AMN species, but not the larger ones, was detected as a soluble molecule in the supernatant fraction of canine renal cortex membranes (prior to detergent solubilization) similarly isolated by IF-cobalamin affinity chromatography (Figure 2 lane 5). Peptide mapping of the approximately 48-kDa AMN species identified the same peptides as indicated and the additional peptides 294-318, 322-342, 343-362, 401-428, and 429-445 composing 53% of the entire mature protein, and this species reacted with the AMN antiserum directed at the intracellular tail peptide. There was insufficient material for peptide mapping of the approximately 43-kDa AMN species, but it also reacted with the AMN antiserum directed at the intracellular tail peptide (Figure 2 lane 3). Thus, the approximately 40-kDa AMN species is apparently truncated within or just extracellular to the transmembrane domain and the approximately 48-kDa species represents the full-length, N-glycosylated form of AMN.

AMN mutation analysis

AMN cDNA was amplified by RT-PCR from kidney cortex RNA isolated from an affected dog of the GS kindred, and sequencing revealed an in-frame, 33-bp deletion in exon 10, predicting loss of 11 amino acid residues from the transmembrane domain somewhere between residues 370-382 (Figure 3A). The deletion end points could not be determined exactly because they occurred within each of 2 nearly perfect copies of a 24-bp direct repeat sequence separated by 9 bp. A sequence variation of the repeats allowed us to place the 5′ deletion end point on or between nucleotides 1106-1113 of the cDNA sequence and the corresponding 3′ deletion end point on or between nucleotides 1138-1145, and therefore, the mutation is designated c.1113_1145del. Presence of the repeat sequences suggests that the mechanism of deletion was an unequal crossover event after misalignment of the repeats during meiosis I. The same 33-bp deletion in exon 10, but no other sequence variation in exons or intronic consensus splice sites, was found in PCR products amplified from gDNA of affected dogs. Computerized transmembrane domain prediction (http://www.cbs.dtu.dk/services/TMHMM/) returned a probability of 1.0 for a transmembrane domain between amino acid residues 363 and 387 of the normal sequence, but less than 0.05 for the mutant sequence. The deletion was homozygous in 18 affected dogs, heterozygous in 8 obligate carriers, and was not seen in 224 chromosomes of unrelated healthy dogs of various breeds.

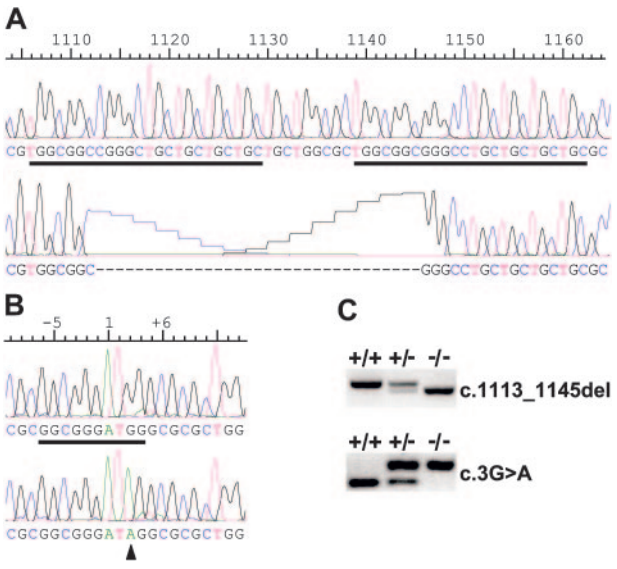

Figure 3. *AMN* mutations in canine I-GS. (A) Normal canine *AMN* cDNA sequence in exon 10 (above) and the corresponding c.1113_1145del mutation sequence of the GS kindred disease allele (below) are shown. Two copies of a near-perfect 24-bp repeat (underlined) apparently predisposed this locus to deletion by unequal crossover. (B) Normal canine *AMN* cDNA sequence in exon 1 (above) and the corresponding c.3G>A mutation sequence (arrowhead) of the AS kindred disease allele (below) are shown. The putative translation initiation site of the normal sequence is underlined and conforms to the Kozak consensus. (C) Representative mutation screening tests performed with gDNA templates are shown.

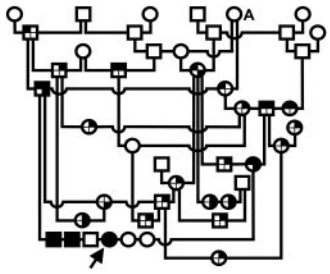

Figure 4. I-GS segregating in an Australian shepherd dog (AS) pedigree. Squares are males and circles are females, and the arrow indicates the proposita. Open and partially filled symbols indicate dogs that were clinically healthy as determined by physical examination, if genotyped, or by family history, if not. Symbols filled in the upper left quadrant indicate dogs that were genotyped at the *KNS2* locus, and symbols filled in the upper right quadrant indicate dogs genotyped for the *AMN* c.3G>A mutation. Symbols filled in the lower right quadrant indicate dogs determined by genotyping to be heterozygous (G/A) at the mutation site. The 3 clinically affected dogs, indicated by symbols filled in all quadrants, were genotyped at both loci and determined to be homozygous A/A at the mutation site. The 2 symbols filled in the lower right but not the upper right quadrant indicate dogs that were inferred from family data to be heterozygous at the mutation site. The female dog labeled A is an ancestor common to all dogs in the kindred determined to be carriers of the c.3G>A *AMN* allele.

A second canine I-GS family (AS kindred; Figure 4) was studied in which 3 affected littermates, 2 male and 1 female born of clinically healthy parents, exhibited growth failure, methylmalonic aciduria, mild nonregenerative anemia, neutropenia, subnormal serum cobalamin concentrations, and low-molecular-weight proteinuria. Parenteral cobalamin administration produced complete remission of the clinical, hematologic, and metabolic disease in 2 of the affected dogs, even though cobalamin malabsorption and proteinuria remained. The third affected dog died at 9 months of age in a state of inappetence, weakness, and extreme emaciation before diagnosis was made. Thus, clinical features of the disorder in the AS kindred were identical to those previously reported for affected dogs of the GS kindred.[11]

A *KNS2* C>T polymorphism that was in complete linkage disequilibrium with *AMN* alleles in the GS kindred[19] segregated with the disorder (logarithm of the odds [LOD] = 1.7, θ = 0.0) when genotyped in 11 members of the AS kindred, including the 3 affected siblings and their parents. RT-PCR amplification of RNA isolated from a renal cortex biopsy of an affected dog revealed a G>A transition at position 3 of the cDNA sequence (c.3G>A), thereby disrupting the Kozak consensus sequence for translation initiation[33] and obliterating a *Bst*F5I recognition sequence (Figure 3B). The mutation was present in gDNA and segregated with the disease allele, as expected for an autosomal recessive disorder, in 3 affected (A/A), 2 obligate carriers (G/A), and 17 other closely related, clinically healthy dogs of the AS kindred (14 G/G and 3 G/A). The mutation was not observed in 120 chromosomes of unrelated healthy dogs of various breeds.

Two clinically healthy dogs of the AS kindred were additionally inferred from the data to be heterozygous for the c.3G>A mutation. One of those was homozygous for the C allele of the *KNS2* polymorphism, and another unaffected dog that did not carry the mutant allele at all was heterozygous at the *KNS2* locus. Thus, the C allele of the *KNS2* polymorphism was of sufficiently high

frequency to have entered the AS pedigree on 2 haplotypes, only one of which was associated with the mutant allele.

AMN null mutations abrogate apical membrane targeting of cubilin in vivo

Full-length *AMN* cDNAs of mutant dogs of both kindreds were readily amplified by RT-PCR, suggesting that RNA transcription, processing, and stability were not greatly affected by the disease mutations. To determine the effect of the c.1113_1145del mutation on protein expression in kidney, the cubam complex was enriched, in bulk, by IF-cobalamin affinity chromatography from pooled fresh frozen kidney of unrelated healthy dogs and affected dogs of the GS kindred. It was evident that certain bands or spots between 37 and 50 kDa were missing from silver-stained or Western blotted 1- or 2-dimensional gels of affected dog proteins when compared with equally loaded (total protein) gels of normal dog proteins (Figure 5A). Proteins of healthy dogs corresponding to those missing from affected dog gels were confirmed as AMN by peptide mapping. To accommodate the small amount of tissue available from an affected dog of the AS kindred, these experiments were repeated in small-scale IF-cobalamin affinity pull-down of proteins followed by Western blot. None of the AMN proteins of normal dog kidney (Figure 5B lane 2) were observed in affected dogs of either kindred (GS, lane 3; AS, lane 4), indicating that the amount of AMN protein participating in cubam complexes expressed by affected dogs in both kindreds was much reduced or nil at steady state and that both the c.1113_1145del and c.3G>A *AMN* mutations were effectively null.

Renal proximal tubule expression of cubilin in the absence of detectable AMN expression was examined by immunohistochemistry. As demonstrated before,[16,17] cubilin immunoreactivity was predominantly at the apical domain of the plasma membrane in proximal tubule epithelial cells of healthy dogs. In sharp contrast, cubilin immunoreactivity was found entirely in an intracellular vesicular pattern in affected dogs in both kindreds, with no detectable labeling of the apical membrane domain (Figure 5C). Apical membrane localization of megalin (gp330, LRP2) in proximal tubule cells was not impaired in affected dogs.[16]

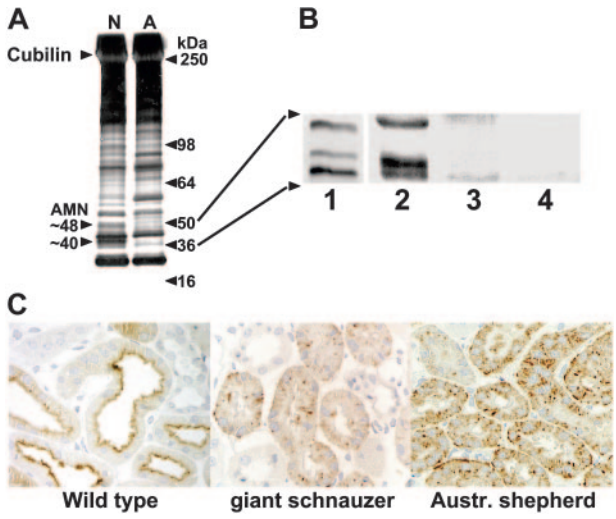

Figure 5. Cubilin and AMN expression in normal and I-GS affected dog kidney in vivo. (A) Membrane fractions prepared in bulk from normal (N) and GS kindred affected (A) dog kidney cortex were detergent solubilized and subjected to IF-cobalamin affinity chromatography. Eluted proteins were concentrated, separated by SDS-PAGE on an 8% to 16% gradient gel, and silver stained. Two bands missing from the affected dog preparation migrated at approximately 48 and 40 kDa (arrowheads) and comigated with anti-AMN immunoreactive bands on Western blots of duplicate gels. They were identified by LC/MS/MS peptide mapping as full-length and C-terminally truncated AMN, respectively. (B) Anti-AMN Western blots of proteins isolated by large-scale IF-cobalamin affinity chromatography from normal dog kidney (lane 1) or by small-scale IF-cobalamin pull-down from kidney cortex homogenates of a normal dog (lane 2), a GS kindred affected dog (lane 3), and an AS kindred affected dog (lane 4). (C) Immunoperoxidase staining of cubilin in renal cortex of an unrelated normal dog (left) and I-GS affected dogs of the GS (middle) and AS (right) kindreds expressing *AMN* mutations c.1113-1145del and c.3G>A, respectively. Total original magnification, 200 ×.

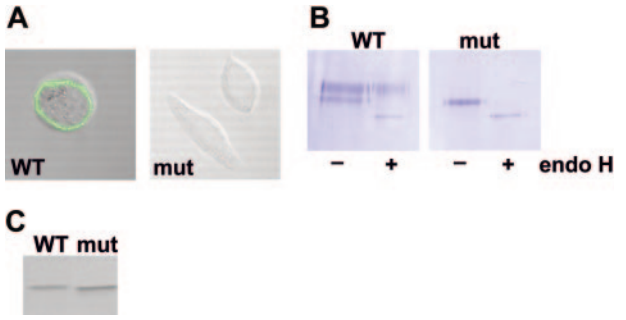

Figure 6. Cubilin expression in CHO cells transfected with wild-type or c.1113-1145del AMN cDNA. (A) CHO cell lines expressing a "mini-cubilin" construct of rat origin were additionally transfected with wild-type (WT) or c.1113-1145del (mut) canine *AMN* cDNA constructs, and stable double transfectants expressing cubilin and AMN were selected. Nonpermeabilized cells were stained for confocal fluorescence microscopy by incubation at 4°C with anticubilin and subsequently with labeled anti–rabbit IgG. Abundant surface staining of cubilin was observed in cells expressing wild-type, but not mutant, *AMN*. (B) Proteins isolated by IF-cobalamin pull-down from lysates of double-transfectant cell lines were subjected to endo H or mock digestion followed by SDS-PAGE and Western blot with anticubilin serum. Golgi maturation of cubilin N-linked oligosaccharides to endo H-resistant forms was observed in cells expressing wild-type AMN, but not in cells expressing the mutant AMN. (C) Lysates of double-transfectant cell lines were subjected to Western blotting with anti-myc, confirming expression of wild-type and mutant AMN.

The *AMN* c.1113_1145del mutation abrogates cubilin processing and membrane targeting in transfected CHO cells

To investigate further the effects of *AMN* null mutations on cubilin expression, we cloned the full-length wild-type and *AMN* c.1113_1145del open reading frames into a previously described[5] *AMN-myc* expression plasmid. CHO cells already expressing a truncated construct of rat cubilin[10] were transfected with one or the other *AMN* construct, and stable double-transfectant cell lines were selected. AMN expression was confirmed by Western blot in both cell lines (Figure 6C). Cells transfected with wild-type canine *AMN* cDNA exhibited the expected surface expression of cubilin, as detected by fluorescent anticubilin labeling and confocal microscopy, but cells transfected with the mutant *AMN* cDNA did not (Figure 6A). Proteins from each cell line were isolated on IF-cobalamin affinity beads, subjected to endo H or mock digestion, and Western blotted with anticubilin serum (Figure 6B). In cells expressing wild-type canine *AMN*, cubilin was detected as 2 distinct bands, the larger of which did not exhibit a gel mobility shift after endo H digestion (endo H resistant) and the smaller of which migrated as a smaller species after endo H digestion (endo H sensitive). In contrast, cells expressing the c.1113-1145del mutant *AMN* exhibited cubilin only as a single band that comigrated with the smaller species observed in the wild-type *AMN* cell line and that was endo H sensitive. Thus, cubilin expressed in CHO cells in the absence of functional, wild-type AMN did not progress through the biosynthetic pathway to the stage of oligosaccharide maturation and was not trafficked efficiently to the cell surface.

Discussion

Previous characterization of canine I-GS in the GS kindred demonstrated that cubilin expressed in distal small intestinal and

proximal tubule epithelia of affected dogs does not reach the apical membrane domain and, so, cannot fulfill its endocytic function.[11-17] Endo H sensitivity of kidney cubilin indicated that it had not been exposed to the biosynthetic oligosaccharide processing enzymes of the Golgi apparatus, and limited proteolytic digestion suggested that the protein was incompletely folded.[12] Those in vivo findings are now attributable to the *AMN* c.1113-1145del mutation and are identical to the observations here that cubilin expressed in CHO cells expressing *AMN* c.1113-1145del did not reach the plasma membrane and, as indicated by endo H sensitivity, was retained in a pre-Golgi biosynthetic compartment. In contrast to *AMN* expression in affected dog kidney in vivo, when *AMN* c.1113-1145del was overexpressed in CHO cells, the mutant protein was readily detectable but was no more capable of shepherding cubilin to the cell membrane than when cells were transfected with no *AMN* construct.[10]

The failure of apical membrane cubilin expression was demonstrated here in I-GS caused by a second *AMN* mutation. The *AMN* c.3G>A mutation of the AS kindred obliterates the translation initiation codon and is an obvious null mutation, as further evidenced by failure to detect AMN on Western blots of AS affected dog kidney. Although the *AMN* c.1113-1145del gene product may be translated, it is likely that the deleted product does not fold properly in vivo and is undetectable on Western blots of kidney proteins because it is targeted for rapid degradation. Thus, in kidney of both kindreds, effectively null *AMN* mutations block trafficking of cubilin to the apical plasma membrane and, thereby, all cubam-mediated endocytic functions. These findings are compatible with an active quality-control function of the RER in proximal tubule cells and suggest that cubilin and AMN must interact in the RER for protein stability and to become competent for exit from RER and apical membrane targeting.

What is the genesis of 3 AMN isoforms observed on Western blots of normal dog kidney proteins? Each had an intact amino terminus and as much of extracellular domain structure as necessary for binding to cubilin during affinity isolation and reaction with anti–extracellular peptide sera. The identities of 2 were confirmed by LC/MS/MS peptide mapping, the largest representing the full-length translation product and the smallest lacking membrane anchorage and the entire intracellular domain. Alternative splicing of known exons does not explain these data. Although possible, the short isoforms are probably not simply the result of nonspecific ex vivo proteolysis because the source tissue was immediately snap frozen, a precaution that was not possible in previous studies of human cadaver kidney where the same multiple isoforms were observed.[10] Thus it appears that the successively smaller AMN isoforms were derived from progressive carboxy-terminal truncation of the full-length translation product that may be due to as yet undefined posttranslational or postendocytic modifications of unknown physiologic significance. Curiously, there is a furin cleavage site in the juxtamembrane portion of the cytoplasmic domain that is conserved in the mammalian AMN proteins. Cleavage at this site would produce an isoform of the observed approximately 43 kDa and basic pI, but the catalytic domains of enzymes in the proprotein convertase family, including furin, described to date are exposed to the noncytoplasmic compartment of Golgi cisternae, secretory vesicles, and endocytic pathway vesicles and should not have access to the cytoplasmic tail of AMN.

From phylogenetic analysis it appears that AMN functions have been sufficiently important through evolution, from insects to mammals, to maintain nearly identical structural and functional components of the protein. In the genome sequence of each species where an *AMN* ortholog was found, a full-length *CUBN* ortholog was also found. However, orthologs of IF were found only in the mammalian species, so it is likely that functions other than IF-cobalamin absorption from intestine have provided a selective advantage for cubam conservation. Additionally intriguing is the apparent expression of *AMN* in tissues where *CUBN* is not, suggesting that there are as yet unsuspected AMN functions. However, despite demonstration here and elsewhere of *CUBN* or *AMN* expression in those tissues,[34-37] no aspect of the I-GS phenotype in humans or dogs has yet been attributed to malfunction of cubilin or AMN in any tissue other than intestine and kidney.

In mice, tissue expression of AMN includes the extraembryonic visceral endoderm, and *AMN* knockout mutations cause early embryonic malformation and death.[9] Cubilin is expressed in the same early embryonic structure of mice,[37] and exposure of developing rat embryos to anticubilin antibodies causes embryonic malformations and lethality.[38] Although undefined as yet, cubilin and AMN probably collaborate in an essential endocytic function in rodent embryonic tissue that is not required or is performed by a redundant mechanism during human and canine embryogenesis. More recently, construction of mouse blastocyst chimeras rescued the lethal phenotype of $Amn^{-/-}$ mice and demonstrated that cubilin was not trafficked to the apical surface of cells derived from the $Amn^{-/-}$ embryonic stem cells in fetal and adult tissues.[39]

Finally, a volume of literature demonstrates that cubilin has a functional relationship with megalin (gp330, LRP2) another large, multiligand endocytic receptor of polarized epithelia.[8,15,40] The 2 receptors colocalize in the apical membrane endocytic apparatus, show partial overlap of expressing tissues, and appear to collaborate in the endocytosis of certain ligands. Moreover, renal cubilin expression is impaired in megalin knockout mice, and renal expression of both receptors is impaired in the proximal tubule chloride channel (ClC-5) knockout mouse ($Clcn5^{-/Y}$).[41] Thus, the enunciated dual-receptor concept (megalin + cubilin) may still have validity if modified (megalin + cubam) to recognize that cubilin expression and function rely on AMN, at least in kidney, intestine, and mouse embryonic tissues. As previously suggested, AMN may direct proper folding, apical membrane trafficking, and initial interaction of cubam with the endocytic apparatus, whereas megalin could exert an important influence elsewhere, such as on cubam recycling or endosome integrity.[40]

Studies of I-GS dogs conclusively demonstrate that effective cubam expression does not occur in the absence of AMN. Cubilin and AMN thus join a small but growing group of membrane receptors that specifically rely on the accessory activity of a separate gene product for trafficking and membrane expression.[42,43] Although studies of AMN and cubilin expression in human I-GS are not likely to be done directly, the heterologous expression system used here recapitulates the essential aspects of cubam expression, regardless of the *AMN* or *CUBN* species origin. Therefore, this system can be used to investigate interesting human *AMN* and *CUBN* mutations and to determine the molecular domains of AMN and cubilin involved in their interaction. We continue to ascertain new canine I-GS kindreds with the prospect of finding additional genes or protein interactions involved in cubam expression and function.

Acknowledgments

The authors thank K. Lassen (deceased), G. Biller, and Z. Li for valued technical assistance and P. Verroust for fruitful discussion. The coauthor Mette Madsen has previously published under the name Mette Kristiansen.

References

1. Rosenblatt DS, Fenton WA. Inborn errors of cobalamin metabolism. In: Banerjee R, ed. Chemistry and Biochemistry of Vitamin B_{12}. New York, NY: John Wiley and Sons; 1999:367-384.
2. Imerslund O. Idiopathic chronic megaloblastic anemia in children. Acta Paediatr Scand. 1960; 49(suppl 119):1-115.
3. Gräsbeck R, Gordin R, Kantero I, Kuhlback B. Selective vitamin B_{12} malabsorption and proteinuria in young people. Acta Med Scand. 1960;167: 289-296.
4. Aminoff M, Carter JE, Chadwick RB, et al. Mutations in *CUBN*, encoding the intrinsic factor-vitamin B_{12} receptor, cubilin, cause hereditary megaloblastic anaemia 1. Nat Genet. 1999;21:309-313.
5. Tanner SM, Aminoff M, Wright FA, et al. Amnionless, essential for mouse gastrulation, is mutated in recessive hereditary megaloblastic anemia. Nat Genet. 2003;33:426-429.
6. Tanner SM, Li Z, Bisson R, et al. Genetically heterogeneous selective intestinal malabsorption of vitamin B_{12}: founder effects, consanguinity, and high clinical awareness explain aggregations in Scandinavia and the Middle East. Hum Mutat. 2004;23:327-333.
7. Tanner SM, Zhongyuan L, Perko JD, et al. Hereditary juvenile cobalamin deficiency caused by mutations in the intrinsic factor gene. Proc Natl Acad Sci U S A. 2005;102:4130-4133.
8. Christensen EI, Birn H. Megalin and cubilin: multifunctional endocytic receptors. Nat Rev Mol Cell Biol. 2002;3:256-266.
9. Kalantry S, Manning S, Haub O, et al. The amnionless gene, essential for mouse gastrulation, encodes a visceral-endoderm-specific protein with an extracellular cysteine-rich domain. Nat Genet. 2001;27:412-416.
10. Fyfe JC, Madsen M, Højrup P, et al. The functional cobalamin (vitamin B_{12})-intrinsic factor receptor is a novel complex of cubilin and amnionless. Blood. 2004;103:1573-1579.
11. Fyfe JC, Giger U, Hall CA, et al. Inherited selective intestinal cobalamin malabsorption and cobalamin deficiency in dogs. Pediatr Res. 1991;29: 24-31.
12. Fyfe JC, Ramanujam KS, Ramaswamy K, Patterson DF, Seetharam B. Defective brush-border expression of intrinsic factor-cobalamin receptor in canine inherited intestinal cobalamin malabsorption. J Biol Chem. 1991;266:4489-4494.
13. Xu D, Fyfe JC. Cubilin expression and posttranslational modification in the canine gastrointestinal tract. Am J Physiol Gastrointest Liver Physiol. 2002;279:G748-G756.
14. Nykjaer A, Fyfe JC, Kozyraki R, et al. Cubilin dysfunction causes abnormal metabolism of the steroid hormone 25(OH) vitamin D_3. Proc Natl Acad Sci U S A. 2001;98:13895-13900.
15. Kozyraki R, Fyfe J, Verroust PJ, et al. Megalin-dependent cubilin-mediated endocytosis is a major pathway for uptake of transferrin in polarized epithelia. Proc Natl Acad Sci U S A. 2001;98: 12491-12496.
16. Birn H, Fyfe J, Jacobsen C, et al. Cubilin is an albumin binding protein important for renal albumin reabsorption. J Clin Invest. 2000;105:1353-1361.
17. Kozyraki R, Fyfe J, Kristiansen M, et al. The intrinsic factor vitamin B_{12} receptor, cubilin, is a novel high affinity apolipoprotein A-1 receptor facilitating endocytosis of high-density lipoprotein. Nat Med. 1999;5:656-661.
18. Xu D, Kozyraki R, Newman TC, Fyfe JC. Genetic evidence of an accessory protein activity required specifically for cubilin brush-border expression and intrinsic factor-cobalamin absorption. Blood 1999;94:3604-3606.
19. He Q, Fyfe JC, Schäffer AA, Werner P, Kirkness EF, Henthorn PS. Canine Imerslund-Gräsbeck syndrome maps to a region orthologous to HSA14q. Mamm Genome 2003;14:758-764.
20. Kawasaki ES. Sample preparation from blood, cells, and other fluids. In: Innis MA, Gelfand DH, Sninsky JJ, White TJ, eds. PCR Protocols: Guide to Methods and Applications. San Diego, CA: Academic Press; 1990:146-152.
21. Sambrook J, Fritsch EF, Maniatis R. Molecular Cloning. A Laboratory Manual. 2nd ed. Cold Spring Harbor, NY: Cold Spring Harbor Laboratory Press; 1989:9.16-9.19.
22. Cottingham RW Jr, Idury RM, Schäffer AA. Faster sequential genetic linkage computations. Am J Hum Genet. 1993;53:252-263.
23. Schäffer AA, Gupta SK, Shriram K, Cottingham RW Jr. Avoiding recomputation in linkage analysis. Human Hered. 1994;44:225-237.
24. Lathrop GM, Lalouel J-M, Julier C, Ott J. Strategies for multilocus analysis in humans. Proc Natl Acad Sci U S A. 1984;81:3443-3446.
25. Ray J, Bouvet A, DeSanto C, et al. Cloning of the canine β-glucuronidase cDNA, mutation identification in canine MPS VII, and retroviral vector-mediated correction of MPS VII cells. Genomics. 1998;48:248-253.
26. Israel DI. A PCR-based method for high stringency screening of DNA libraries. Nucleic Acid Res. 1993;21:2627-2631.
27. Birn H, Verroust PJ, Nexø E, et al. Characterization of an epithelial approximately 460-kDa protein that facilitates endocytosis of intrinsic factor-vitamin B_{12} and binds receptor-associated protein. J Biol Chem. 1997;272:26497-26504.
28. Celis JE, Ratz G, Basse B, Lauridsen JB, Celis A. High-resolution two-dimensional gel electrophoresis of proteins: isoelectric focusing and nonequilibrium pH gradient electrophoresis (NEPHGE). In: Celis JE, ed. Cell Biology: A Laboratory Handbook. Vol 4. New York, NY: Academic Press; 1994: 222-230.
29. Mørtz E, Krogh TN, Vorum H, Gorg A. Improved silver staining protocols for high sensitivity protein identification using matrix-assisted laser desorption/ionization-time of flight analysis. Proteomics. 2001;1:359-1363.
30. Froehlich JE, Wilkerson CG, Ray WK, et al. Proteomic study of the *Arabidopsis thaliana* chloroplastic envelope membrane utilizing alternatives to traditional two-dimensional electrophoresis. J Proteome Res. 2003;2:413-425.
31. Perkins DN, Pappin DJ, Creasy DM, Cottrell JS. Probability-based protein identification by searching sequence databases using mass spectrometry data. Electrophoresis. 1999;20:3551-3567.
32. Boll W, Rapoport I, Brunner C, et al. The μ2 subunit of the clathrin adaptor AP-2 binds to FD-NPVY and YppØ sorting signals at distinct sites. Traffic. 2002;3:590-600.
33. Kozak M. Emerging links between initiation of translation and human diseases. Mamm Genome. 2002;13:401-410.
34. Kolleck I, Wissel H, Guthmann F, et al. HDL-holoparticle uptake by alveolar type II cells: effect of vitamin E status. Am J Respir Cell Mol Biol. 2002; 27:57-63.
35. Crider-Pirkle S, Billingsley P, Faust C, et al. Cubilin, a binding partner for galectin-3 in the murine utero-placental complex. J Biol Chem. 2002;277: 15904-15912.
36. Erranz B, Miquel JF, Argraves WS, et al. Megalin and cubilin expression in gallbladder epithelium and regulation by bile acids. J Lipid Res. 2004;45: 2185-2198.
37. Drake CJ, Fleming PA, Larue AC, Barth JL, Chintalapudi MR, Argraves WS. Differential distribution of cubilin and megalin expression in the mouse embryo. Anat Rec. 2004;277A:163-170.
38. Sahali D, Mulliez N, Chatelet F, Dupuis R, Ronco P, Verroust P. Characterization of a 280-kD protein restricted to the coated pits of the renal brush border and the epithelial cells of the yolk sac. Teratogenic effect of the specific monoclonal antibodies. J Exp Med. 1988;167:213-218.
39. Strope S, Rivi R, Metzger T, Manova K, Lacy E. Mouse amnionless, which is required for primitive streak assembly, mediates cell-surface localization and endocytic function of cubilin on visceral endoderm and kidney proximal tubules. Development. 2004;131:4787-4795.
40. Müller D, Nykjaer A, Willnow TE. From holoprosencephaly to osteopathology: role of multifunctional endocytic receptors in absorptive epithelia. Ann Med. 2003;35:290-299.
41. Christensen EI, Devuyst O, Dom G, et al. Loss of chloride channel ClC-5 impairs endocytosis by defective trafficking of megalin and cubilin in kidney proximal tubules. Proc Natl Acad Sci U S A. 2003;100:8472-8477.
42. Metherell LA, Chapple JP, Cooray S, et al. Mutations in *MRAP*, encoding a new interacting partner of the ACTH receptor, cause familial glucocorticoid deficiency type 2. Nat Genet. 2005; 37:166-170.
43. Saito H, Kubota M, Roberts RW, Chi Q, Matsunami H. RTP family members induce functional expression of mammalian odorant receptors. Cell. 2004;119:679-691.